Article

Electronic and Steric Effects on Molecular Dihydrogen Activation in [Cp*OsH(L)] (L = PPh, AsPh, and PCy)

Charles Edwin Webster, Christopher L. Gross, Dianna M. Young, Gregory S. Girolami, Arthur J. Schultz, Michael B. Hall, and Juergen Eckert

J. Am. Chem. Soc., **2005**, 127 (43), 15091-15101• DOI: 10.1021/ja052336k • Publication Date (Web): 08 October 2005

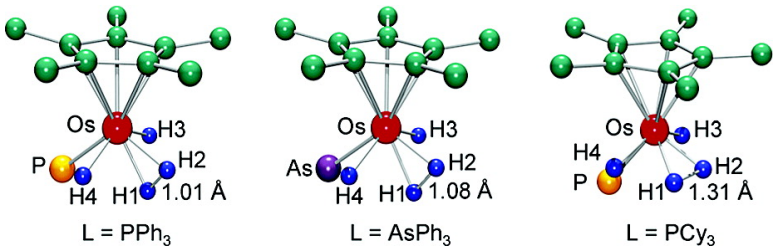

More About This Article

Additional resources and features associated with this article are available within the HTML version:

- Supporting Information
- Links to the 3 articles that cite this article, as of the time of this article download
- Access to high resolution figures
- Links to articles and content related to this article
- Copyright permission to reproduce figures and/or text from this article

View the Full Text HTML

Journal of the American Chemical Society is published by the American Chemical Society. 1155 Sixteenth Street N.W., Washington, DC 20036

J|A|C|S
ARTICLES
Published on Web 10/08/2005

Electronic and Steric Effects on Molecular Dihydrogen Activation in $[Cp^*OsH_4(L)]^+$ (L = PPh_3, $AsPh_3$, and PCy_3)

Charles Edwin Webster,[†,⊥] Christopher L. Gross,[‡] Dianna M. Young,[¶] Gregory S. Girolami,*[,‡] Arthur J. Schultz,*[,¶] Michael B. Hall,*[,†] and Juergen Eckert*[,§]

Contribution from the School of Chemical Sciences, The University of Illinois at Urbana−Champaign, 600 South Mathews Avenue, Urbana, Illinois 61801, Intense Pulsed Neutron Source, Argonne National Laboratory, Argonne, Illinois 60439, Department of Chemistry, Texas A&M University, Ross and Spence Streets, P.O. Box 30012, College Station, Texas 77842-3012, Los Alamos Neutron Science Center, Mail Stop H805, Los Alamos National Laboratory, Los Alamos, New Mexico 87545, and Materials Research Laboratory, University of California, Santa Barbara, California 93106

Received April 11, 2005; E-mail: girolami@scs.uiuc.edu

Abstract: Single-crystal neutron diffraction, inelastic neutron scattering, and density functional calculations provide experimental and theoretical analyses of the nature of the osmium-bound, "elongated" dihydrogen ligands in $[Cp^*OsH_4(L)][BF_4]$ complexes (L = PPh_3, $AsPh_3$, or PCy_3). The PPh_3 and $AsPh_3$ complexes clearly contain one dihydrogen ligand and two terminal hydrides; the H_2 ligand is transoid to the Lewis base, and the H−H vector connecting the central two hydrogen atoms lies parallel to the Ct−Os−L plane (Ct = centroid of Cp* ring). In contrast, in the PCy_3 complex the H−H vector is perpendicular to the Ct−Os−L plane. Not only the orientation of the central two hydrogen atoms but also the H−H bond length between them depends significantly on the nature of L: the H···H distance determined from neutron diffraction is 1.01(1) and 1.08(1) Å for L = PPh_3 and $AsPh_3$, respectively, but 1.31(3) Å for L = PCy_3. Density functional calculations show that there is a delicate balance of electronic and steric influences created by the L ligand that change the molecular geometry (steric interactions between the Cp* and L groups most importantly change the Ct−Os−L angle), changing the relative energy of the Os 5d orbitals, which in turn govern the H−H distance, preferred H−H orientation, and rotational dynamics of the elongated dihydrogen ligand. The geometry of the dihydrogen ligand is further tuned by interactions with the BF_4^- counterion. The rotational barrier of the bound H_2 ligand in $[Cp^*OsH_4(PPh_3)]^+$, determined experimentally (3.1 kcal mol^{-1}) from inelastic neutron scattering experiments, is in reasonable agreement with the B3LYP calculated H_2 rotational barrier (2.5 kcal mol^{-1}).

Introduction

Since their discovery, molecular dihydrogen complexes have generated considerable interest because they give a direct view of the intermediate (or transition state) that lies along the reaction coordinate for the oxidative addition of dihydrogen to transition-metal centers (Scheme 1).[1] The H···H bond distance is often used as a measure of the extent to which the H_2 ligand has been activated. Distances less than 0.90 Å are typical for "normal" dihydrogen complexes, whereas distances longer than 1.50 Å are characteristic of classical dihydride complexes.[1e] A few dihydrogen complexes, however, constitute an intermediate situation with "elongated" H···H bonds of approximately 1.0−1.4 Å.[1e]

Scheme 1. Activation of H_2 by a Transition Metal Complex

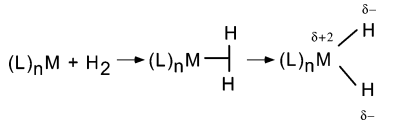

In 1999, we reported the synthesis of two osmium dihydrogen complexes, $[Cp^*OsH_4(PPh_3)][BF_4]$ (**1**) and $[Cp^*OsH_4(AsPh_3)][BF_4]$ (**2**), where Cp* is η^5-C_5Me_5.[2] A preliminary single-crystal neutron diffraction study of **1** revealed that two of the hydride ligands (those transoid to the Lewis base, L) form an "elongated" dihydrogen ligand. We now describe full details of the structures of these two complexes, along with that of the tri(cyclohexyl)-phosphine analogue $[Cp^*OsH_4(PCy_3)][BF_4]$ (**3**). Interestingly, the H_2 ligand in the latter molecule is oriented differently than those in complexes **1** and **2**: whereas the H_2 ligand vector lies

[†] Texas A&M University.
[‡] The University of Illinois at Urbana−Champaign.
[¶] Argonne National Laboratory.
[§] Los Alamos National Laboratory and University of California, Santa Barbara.
[⊥] Present address: Department of Chemistry, The University of Memphis, 213 Smith Chemistry Building, Memphis, TN 38152-3550.

(1) (a) Heinekey, D. M.; Oldham, W. J. *Chem. Rev.* **1993**, *93*, 913−926. (b) Jessop, P. G.; Morris, R. H. *Coord. Chem. Rev.* **1992**, *121*, 155−284. (c) Kubas, G. J. *Acc. Chem. Res.* **1988**, *21*, 120−128. (d) Morris, R. H. *Can. J. Chem.* **1996**, *74*, 1907−1915. (e) Kubas, G. J. *Metal−Dihydrogen and σ-Bond Complexes: Structure, Theory, and Reactivity*; Kluwer Academic Publishers: Norwell, MA, 2000.

(2) Gross, C. L.; Young, D. M.; Schultz, A. J.; Girolami, G. S. *J. Chem. Soc., Dalton Trans.* **1997**, 3081−3082.

parallel to the Ct−Os−L plane for L = PPh_3 and $AsPh_3$, it lies perpendicular to the Ct−Os−L plane for L = PCy_3. In addition, the H···H distance (determined from neutron diffraction) also depends on the nature of L, being 1.01(1) and 1.08(1) Å for L = PPh_3 and $AsPh_3$, respectively, but 1.31(3) Å for L = PCy_3. These structural differences are provocative because they illustrate that the geometry of a molecular dihydrogen ligand can exhibit an unusual sensitivity to the nature of the ancillary ligands. As such, the exact steric and electronic reasons for the differences are important to elucidate.

The current study combines experimental and theoretical analyses of the electronic and steric influence of these substituted phosphine and arsine ligands on the H···H distance, preferred orientation, and rotational dynamics of the "elongated" dihydrogen ligands in $[Cp^*OsH_4(L)]^+$ (where L = PPh_3, $AsPh_3$, and PCy_3; compounds **1**, **2**, and **3**, respectively). In particular, this work reports (1) single-crystal neutron diffraction studies of **1**−**3**, (2) the inelastic neutron scattering vibrational spectra of the protio and tetradeuterio isotopologues of the PPh_3 complex **1**, and (3) theoretical calculations on both observed and unobserved isomers of $[Cp^*OsH_4(PPh_3)]^+$ and $[Cp^*OsH_4(PCy_3)]^+$.

Experimental and Theoretical Methods

Syntheses. The three compounds $[Cp^*OsH_4(L)][BF_4]$, where L = PPh_3, $AsPh_3$, or PCy_3, were prepared as described previously.[2] The tetradeuterio isotopologue $[Cp^*OsD_4(PPh_3)][BF_4]$ was made from the appropriately deuterated starting materials.

Neutron Diffraction Data Collection and Analysis. Time-of-flight neutron diffraction data were obtained at the Intense Pulsed Neutron Source (IPNS) at Argonne National Laboratory on a single-crystal diffractometer equipped with a position-sensitive ^{6}Li-glass scintillation area (30 × 30 cm^2) detector.[3] At the IPNS, pulses of protons are accelerated into a heavy-element target 30 times per second to produce pulses of neutrons by the spallation process. Due to the pulsed nature of the source, neutron wavelengths are determined by time-of-flight based on the de Broglie equation $\lambda = (h/m)(t/l)$, where h is Planck's constant, m is the neutron mass, and t is the time-of-flight for a flight path l, so that the entire thermal spectrum of neutrons can be used. With a position-sensitive area detector and a range of neutron wavelengths, a solid volume of reciprocal space is sampled with a stationary orientation of the sample and the detector. Details of the data collection and analysis procedures have been provided previously.[4] Table 1 contains a summary of the data collection, analysis, and refinement parameters for compounds **1**−**3**.

Crystals with approximate volumes of 2−5 mm^3 were epoxied to aluminum pins and mounted on the cold stage of a Displex closed-cycle helium refrigerator (Air Products and Chemicals, Inc., model CS-202). In each case an orientation matrix was initially obtained by an auto-indexing procedure applied to data obtained by searching a histogram for peaks.[5] Approximately 25 diffractometer settings were used for the two monoclinic data collections and 50 diffractometer settings for the triclinic crystal to obtain at least one unique octant or hemisphere, respectively, of reciprocal space. For each setting of the diffractometer angles, data were stored in three-dimensional histogram form with coordinates x,y,t corresponding to horizontal and vertical detector positions and the time-of-flight, respectively. The 120 time-of-flight histogram channels were constructed with constant $\Delta t/t$ = 0.015 and correspond to wavelengths of 0.7−4.2 Å. Bragg reflections were integrated about their predicted location and were corrected for the Lorentz factor, the incident spectrum, and the detector efficiency.

Table 1. Crystal and Structural Refinement Data for $[Cp^*OsH_4(L)][BF_4]$ Compounds

	L = PPh_3 (**1**)	L = $AsPh_3$ (**2**)	L = PCy_3 (**3**)
temperature, K	20	20	20
crystal system	monoclinic	monoclinic	triclinic
space group	$P2_1/c$	$P2_1/c$	$P\bar{1}$
a, Å	10.4294(16)	10.5910(16)	8.8096(16)
b, Å	27.562(4)	27.769(4)	9.6314(18)
c, Å	9.4129(4)	9.2920(13)	17.144(3)
α, deg	90	90	94.185(16)
β, deg	99.690(10)	99.610(10)	90.014(15)
γ, deg	90	90	101.385(16)
V, $Å^3$	2641(1)	2694.4(7)	1422.1(5)
Z	4	4	2
data collection techn	TOF Laue with position-sensitive area detector		
radiation	neutrons		
wavelength range, Å	0.7−4.2		
$\mu(\lambda)$, cm^{-1}	1.603λ + 1.319	1.603λ + 1.319	1.908λ + 1.664
reflns with $I > 3\sigma(I)$	3581	2761	2197
no. of variables	324	313	308
$R(F)$	0.088	0.091	0.129
$wR(F)$	0.058	0.057	0.075
GOF	1.66	1.77	1.72

A wavelength-dependent spherical absorption correction was applied using cross sections from Sears[6] for the non-hydrogen atoms and from Howard et al.[7] for the hydrogen atoms. Symmetry-related reflections were not averaged because different extinction factors were applicable to reflections measured at different wavelengths. The structure was refined with the GSAS program.[8] The initial model for each crystal was obtained from structure solutions based on single-crystal X-ray data. In the final refinement, a secondary extinction correction, type I, was included. For the PPh_3 complex **1**, the two hydride and the two dihydrogen atoms were refined anisotropically, and all other atoms were refined isotropically. For the $AsPh_3$ complex **2** and the PCy_3 complex **3**, the data-to-parameter ratios were smaller and more constraints were applied. For **2**, all atoms were refined isotropically; for **3**, many of the temperature factors for chemically similar atoms were constrained to be equivalent, and soft constraints on typical C−C and C−H bond lengths were introduced for the cyclohexyl groups and the cyclopentadienyl ligand.

Inelastic Neutron Scattering. Vibrational spectra of the protio compound, $[Cp^*OsH_4(PPh_3)][BF_4]$, and its tetradeuterio isotopologue, $[Cp^*OsD_4(PPh_3)][BF_4]$, were collected at 20 K on the FDS instrument and inverse-geometry neutron time-of-flight spectrometer[9] at the Lujan Center of Los Alamos National Laboratory. Approximately 1 g of each sample was sealed under a He atmosphere in Al sample containers, which were then mounted in a closed-cycle He refrigerator. The raw data were normalized to the incident neutron spectrum and corrected for the instrumental response function by means of a numerical deconvolution.[10] Theoretical INS spectra were computed with the aid of the program CLIMAX[11] from the frequencies and atomic vibrational amplitudes of the Gaussian98/03 calculations. The only adjustable parameters in this calculation relate to instrumental factors.

Theoretical Calculations. The theoretical calculations were carried out using the Gaussian98[12] and Gaussian03[13] implementations of

(3) Schultz, A. J. *Trans. Am. Crystallogr. Assoc.* **1987**, *23*, 61−69.
(4) Schultz, A. J.; Van Derveer, D. G.; Parker, D. W.; Baldwin, J. E. *Acta Crystallogr. C* **1990**, *46*, 276−279.
(5) Jacobson, R. A. *J. Appl. Crystallogr.* **1986**, *19*, 283−286.
(6) Sears, V. F. In *Neutron Scattering Lengths and Cross Sections*; Sköld, K., Price, D. L., Eds.; Academic Press: Orlando, FL, 1986; pp 521−550.
(7) Howard, J. A. K.; Johnson, O.; Schultz, A. J.; Stringer, A. M. *J. Appl. Crystallogr.* **1987**, *20*, 120−122.
(8) Larson, A. C.; Von Dreele, R. B. General Structure Analysis System−GSAS, Los Alamos National Laboratory, 1994.
(9) Taylor, A. D.; Wood, E. J.; Goldstone, J. A.; Eckert, J. *Nucl. Instrum. Methods Phys. Res.* **1984**, *221*, 408−418.
(10) Sivia, D. S.; Vorderwisch, P.; Silver, R. N. *Nucl. Instrum. Methods A* **1990**, *290*, 492−498.
(11) Kearley, G. J. *Nucl. Instrum. Methods A* **1995**, *354*, 53−58.
(12) Frisch, M. J.; et al. *Gaussian 98*, Revisions A.6, A.7, A.9, and A11.3; Gaussian, Inc.: Pittsburgh, PA, 1998.
(13) Frisch, M. J.; et al. *Gaussian 03*, Revisions B.03 and B.05; Gaussian, Inc., Wallingford, CT, 2004.

B3LYP [the Becke three-parameter exchange functional (B3)[14] and the Lee−Yang−Parr correlation functional (LYP)[15]] density functional theory[16] with the default pruned fine grids for energies (75, 302), default pruned course grids for gradients and Hessians (35, 110) [neither grid is pruned for osmium], and default SCF convergence for geometry optimizations (10^{-8}). The basis set for osmium (341/341/21/1) in all calculations consisted of the effective core potentials (ECP) of Hay and Wadt (LanL2DZ)[17] as modified by Couty and Hall (341/341/21), in which the two outermost p functions are replaced by a (41) split of the optimized osmium 6p function,[18] supplemented with a single set of f polarization functions.[19a] The standard LanL2DZ basis set was used for phosphorus[17] supplemented with a single set of d polarization functions.[19] BS1 utilized the D95** basis sets of Dunning[20] for metal-ligated carbon and hydrogen atoms, the D95 basis set[20] for the carbon atoms directly connected to phosphorus and for the methyl carbon atoms of the Cp* ligand, and the STO-3G basis sets[21] for all other peripheral carbon and hydrogen atoms (the D95** basis sets were used for boron and fluorine, when present). BS2 replaces the basis set for the metal-ligated carbon atoms with a correlation-consistent double-ζ plus polarization basis set (cc-pVDZ)[22] and replaces the metal-ligated hydrogen atoms with a triple-ζ plus double polarization basis set (cc-pVTZ).[22] BS3 utilized the osmium basis set of BS1 and the metal-ligated carbon basis set of BS2 and replaces the metal-ligated hydrogen basis set with cc-pVDZ,[22] the phosphorus basis set with LanL2DZ(d,p),[23] and all other carbon and hydrogen basis sets with D95V (the cc-pVDZ basis sets were used for boron and fluorine, when present).[20] BS4 utilized the osmium basis set of BS1 and the phosphorus basis set, metal-ligated carbon basis set, and all other carbon and hydrogen basis sets of BS3, and replaces the metal-ligated hydrogen basis set with aug-cc-pVQZ.[22] The cc-pVDZ, aug-cc-pVDZ, cc-pVTZ, and aug-cc-pVQZ basis sets have all had the redundant functions removed and have been linearly transformed as suggested by Davidson.[24] Spherical harmonic d and f functions were used throughout; i.e., there are five angular basis functions per d function and seven angular basis functions per f function.

All structures were fully optimized, and analytical frequency calculations were performed on all structures to ensure that either a minimum or first-order saddle point was achieved. The $[Cp^*OsH_4(PCy_3)]^+$ geometry with an elongated H_2 ligand lying perpendicular to the Ct−Os−L plane occupies a shallow minimum, however, and this calculated stationary point (at +1.52 kcal mol^{-1} ΔE) has an imaginary frequency corresponding to the oxidative addition motion leading to the lowest energy tetrahydride structure at 0 kcal mol^{-1}. All reported energies include zero-point energies, unless otherwise noted.

Results and Discussion

Single-Crystal Neutron Diffraction Studies. The inner coordination spheres of the three $[Cp^*OsH_4(L)]^+$ cations with L = PPh_3 (**1**), $AsPh_3$ (**2**), or PCy_3 (**3**), where Cy is cyclohexyl, were determined by single-crystal neutron diffraction (Figure 1). Crystal and structural refinement data are collected in Table 1, and selected distances and angles for the three compounds are summarized in Table 2.

The PPh_3 complex **1** and the $AsPh_3$ complex **2** are isomorphous (monoclinic $P2_1/c$) and nearly isostructural. In both compounds, two of the hydrogen atoms (those transoid to the Lewis base) form a molecular dihydrogen ligand, whereas the two hydrogen atoms cisoid to the Lewis base are classical hydride ligands. Thus, the overall geometry is that of a four-legged piano stool, with the four legs occupied by L, two hydride ligands, and a dihydrogen molecule. For purposes of later discussions, it should be noted that the H_2 ligand (more precisely, the H−H vector connecting these two "central" hydrogen atoms) lies essentially in the Ct−Os−L plane; the relevant torsion angles are all near zero.

The average Os−H distance to the terminal hydride atoms is 1.66(2) Å, and the average Os−H distance to the dihydrogen atoms is 1.67(2) Å. The major differences between **1** and **2** are that the Os−P distance is 0.09 Å shorter than the Os−As bond length (as expected from the relative atomic radii of P and As), and the dihydrogen H(1)−H(2) distance is 1.014(11) Å in the PPh_3 complex but 1.075(13) Å in the $AsPh_3$ complex. The reasons for this 0.06 Å lengthening will be discussed below.

The PCy_3 complex **3** is not isomorphous with **1** and **2**, and instead crystallizes with a triclinic $P\bar{1}$ habit. The most interesting feature of **3** is that the dispositions of the hydrogen atoms differ dramatically from those in **1** and **2**. Although the overall geometry can still be described in terms of a four-legged piano stool, in **3** the H−H vector connecting the two central hydrogen atoms is *perpendicular* to the Ct−Os−L plane. Other differences are apparent: the H(1)−H(2) distance between the two central hydrogen atoms has increased to 1.31(3) Å. The H(1)−H(4) and H(2)−H(3) distances are also reasonably short at 1.55(3) and 1.67(3) Å, respectively. All four hydrogen ligands are nearly coplanar, as shown by the H(4)−H(1)−H(2)−H(3) torsion angle of only 4.9°. In addition, in **3** the Ct−Os−L angle of 139° is about 10° larger than the related angles in **1** and **2**. This difference is probably due to steric crowding between the cyclohexyl groups and the cyclopentadienyl methyl groups (this point will be discussed in detail below).

It has been shown previously that coordinated dihydrogen ligands can act as hydrogen donors in hydrogen-bonding interactions owing to their electropositive character.[25] An examination of the crystal structures shows that the BF_4 counterion forms close H···F contacts with the dihydrogen ligands in **1**−**3**. Specifically, three of the H···F contacts in **1** and **2** are shorter than the sum of the van der Waals radii (2.67 Å), the shortest being H2···F4′ = 2.42 Å in **1** and 2.48 Å in **2**; in contrast, in **3** the shortest H···F contact is 2.74 Å. The intermolecular contacts are consistent with the general trend that dihydrogen ligand atoms are more electropositive than hydride ligands.

Theoretical Results. Density functional calculations were used to optimize the gas-phase structures of the cationic osmium complexes $[Cp^*OsH_4(L)]^+$, where L = PPh_3 or PCy_3, and the results were compared with the solid-state neutron diffraction results. The optimized structures and relative energies of the

(14) Becke, A. D. *J. Chem. Phys.* **1993**, *98*, 5648−5652.
(15) Lee, C.; Yang, W.; Parr, R. G. *Phys. Rev. B* **1988**, *37*, 785−789.
(16) Parr, R. G.; Yang, W. *Density Functional Theory of Atoms and Molecules*; Oxford University Press: New York, 1989.
(17) Hay, P. J.; Wadt, W. R. *J. Chem. Phys.* **1985**, *82*, 270−283. Wadt, W. R.; Hay, P. J. *J. Chem. Phys.* **1985**, *82*, 284−298.
(18) Couty, M.; Hall, M. B. *J. Comput. Chem.* **1996**, *17*, 1359−1370.
(19) (a) Ehlers, A. W.; Böhme, M.; Dapprich, S.; Gobbi, A.; Höllwarth, A.; Jonas, V.; Köhler, K. F.; Stegmann, R.; Veldkamp, A.; Frenking, G. *Chem. Phys. Lett.* **1993**, *208*, 111−114. (b) Höllwarth, A.; Böhme, M.; Dapprich, S.; Ehlers, A. W.; Gobbi, A.; Jonas, V.; Köhler, K. F.; Stegmann, R.; Veldkamp, A.; Frenking, G. *Chem. Phys. Lett.* **1993**, *208*, 237−240; **1994**, *224*, 603.
(20) Dunning, T. H.; Hay, P. J. In *Modern Theoretical Chemistry*; Schaefer, H. F., III, Ed.; Plenum: New York, 1976; pp 1−28.
(21) Hehre, W. J.; Stewart, R. F.; Pople, J. A. *J. Chem Phys.* **1969**, *51*, 2657−2664.
(22) Dunning, T. H. *J. Chem. Phys.* **1989**, *90*, 1007−1023. Woon, D. E.; Dunning, T. H., Jr. *J. Chem. Phys.* **1994**, *100*, 2975−2988.
(23) Check, C. E.; Faust, T. O.; Bailey, J. M.; Wright, B. J.; Gilbert, T. M.; Sunderlin, L. S. *J. Phys. Chem. A* **2001**, *105*, 8111−8116.
(24) Davidson, E. R. *Chem. Phys. Lett.* **1996**, *260*, 514−518.
(25) Albinati, A.; et al. *J. Am. Chem. Soc.* **1993**, *115*, 7300−7312.

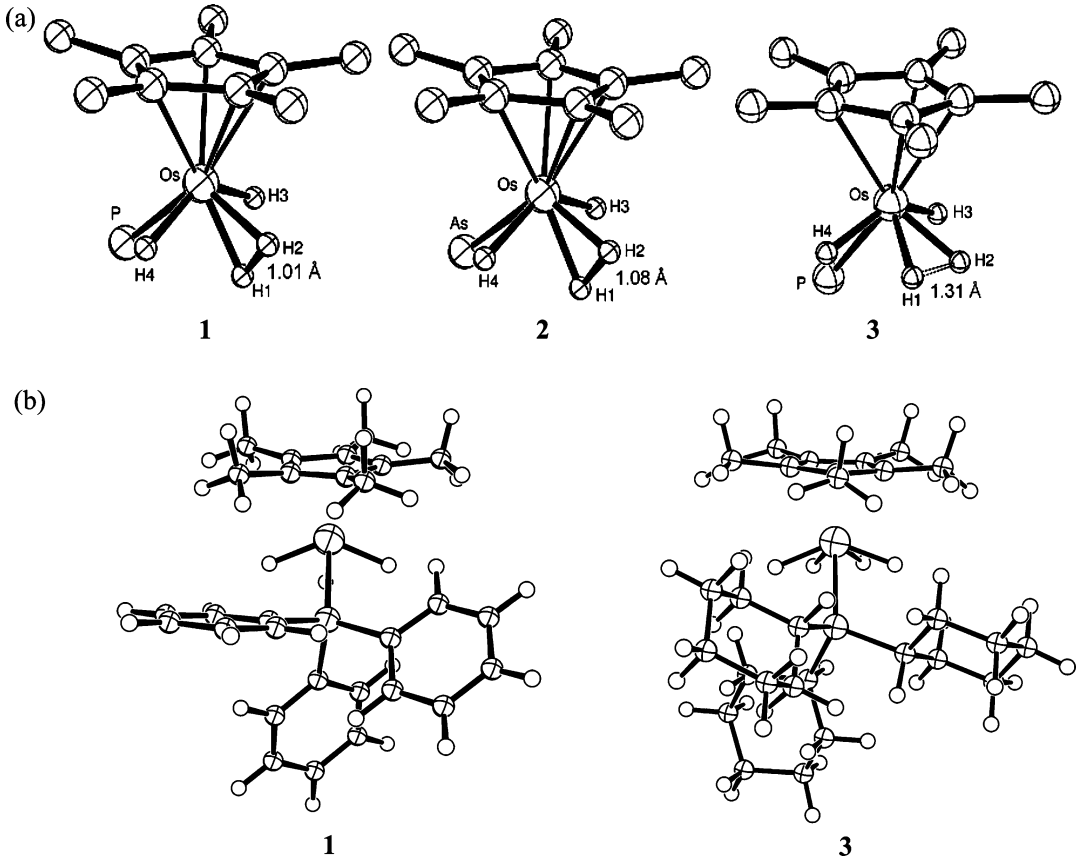

Figure 1. (a) Inner coordination spheres of **1**, **2**, and **3**. The phenyl and cyclohexyl groups bound to phosphorus and arsenic, and the methyl hydrogen atoms on the Cp* ligand, are omitted for clarity. (b) Full structures of **1** and **3** showing the steric interactions between the Cp* ligand and the substituents on the phosphorus ligand. The H_2 ligand in **1** is obscured by the Os and the Os−P bond.

complexes in various low-energy structures, including unobserved isomers, are shown in Figures 2−6.

Four specific angles representing the orientations of the ligands about the osmium will be used to describe and compare the experimental and calculated structures: the Ct−Os−L angle, the C−Ct−Os−L torsion (the C chosen for this torsion angle minimizes the measured angle), the C−Ct−Os angle (this C is the same one used in the C−Ct−Os−L torsion), and the Ct−Os−H(4) angle (Scheme 2).

The most stable calculated structures agree well with the experimental structures (compare Figure 1 with Figures 2−6). For both the gas-phase cationic PPh_3 and PCy_3 complexes, the calculated locations for the two central hydrogen atoms in the lowest energy isomers are slightly different from those determined experimentally by neutron diffraction, but the addition of the BF_4^- counterion brings the structures into closer agreement.

Tetrahydride vs Dihydrogen−Dihydride Gas-Phase Structures. When a polarized double-ζ basis set is employed for the osmium-bound hydrogen atoms (BS1), DFT calculations reveal two minima for the PPh_3 complex **1** with approximately equal energies and generally similar structures (Figure 2). The more stable of these two minima (by 0.53 kcal mol^{-1}) is a classical tetrahydride (**1a** with an H···H distance of 1.50 Å), and the other is a nonclassical dihydrogen−dihydride (**1b** with an H_2 distance of 1.05 Å). In both isomers, the two hydrogen atoms that are "transoid" to the L ligand lie in the Ct−Os−L plane. The experimentally observed structure for **1** corresponds very closely to the latter structure (**1b**); the experimental H_2 distance is 1.01 Å.

Apart from the difference in the H−H distance between the two central hydrogen atoms, there is another significant structural difference between **1a** and **1b**. In the tetrahydride isomer **1a**, the Ct−Os−L angle is 125.8°, whereas in the dihydrogen−dihydride isomer **1b**, the Ct−Os−L angle is 129.8°. Significantly, in the structure determined by neutron diffraction, the Ct−Os−L angle is 129.7°. Thus, the dispositions of the hydrogen atoms (and the presence or absence of a dihydrogen ligand) appear to be correlated with small changes in the angle that the Lewis base forms with the cyclopentadienyl ring.

Replacing the polarized double-ζ basis set on the osmium-bound hydrogen atoms (BS1) with a polarized triple-ζ basis set (BS2) brings the two structures slightly closer in energy (structure **1a** now being lower in energy by only 0.04 kcal mol^{-1}) and leaves the geometric parameters essentially unchanged: the H···H distances are 1.485 and 1.015 Å for the tetrahydride and dihydrogen−dihydride isomers, respectively. An even larger basis set, with quadruple-ζ and polarization and diffuse functions on the osmium-bound hydrogen atoms (BS4), gives virtually identical results for the geometries (H···H of 1.461 and 1.030 Å for the tetrahydride and dihydrogen−dihydride isomers, respectively), now slightly favoring the dihydrogen−dihydride isomer by 0.17 kcal mol^{-1}. (The density functional calculations pertaining to the rotation of the H_2 ligand and the dihydrogen/hydride exchange dynamics in this PPh_3 complex and a comparison to experiment will be described below.)

Table 2. Selected Distances (Å) and Angles (°) for [Cp*OsH_4(L)][BF_4] Compounds

	L = PPh_3 (**1**)	L = $AsPh_3$ (**2**)	L = PCy_3 (**3**)
	Distances[a]		
Os−H(1)	1.659(9)	1.689(9)	1.626(18)
Os−H(2)	1.680(9)	1.649(8)	1.599(21)
Os−H(3)	1.631(9)	1.642(13)	1.632(15)
Os−H(4)	1.654(9)	1.717(15)	1.606(17)
H(1)−H(2)	1.014(11)	1.075(13)	1.306(25)
H(1)−H(3)	1.839(15)	1.872(21)	
H(1)−H(4)	1.929(13)	1.973(17)	1.552(27)
H(2)−H(3)	2.217(15)	2.154(18)	1.670(27)
H(2)−H(4)	2.058(14)	2.153(17)	
H(1)−F(4)	2.546(10)	2.569(12)	2.737(19)
H(2)−F(3)	2.558(10)	2.548(10)	
H(2)−F(4)	2.420(11)	2.479(11)	
Os−L	2.346(5)	2.436(5)	2.357(10)
Os−C(1)	2.276(4)	2.299(5)	2.314(8)
Os−C(2)	2.227(5)	2.233(7)	2.298(8)
Os−C(3)	2.225(5)	2.203(7)	2.232(9)
Os−C(4)	2.259(4)	2.252(5)	2.237(8)
Os−C(5)	2.306(4)	2.307(5)	2.270(8)
	Angles[a]		
Ct−Os−L	129.7	128.5	139.0
Ct−Os−H(1)	147.3	149.9	119.4
Ct−Os−H(2)	112.3	112.4	125.0
Ct−Os−H(3)	114.3	114.4	113.5
Ct−Os−H(4)	113.0	112.3	108.4
L−Os−H(1)	83.0(4)	81.5(4)	95.3(8)
L−Os−H(2)	117.9(4)	119.0(5)	93.4(9)
L−Os−H(3)	74.9(3)	75.5(4)	69.8(7)
L−Os−H(4)	77.3(3)	77.1(4)	71.6(7)
H(1)−Os−H(2)	35.4(4)	37.5(5)	47.8(9)
H(1)−Os−H(3)	68.0(5)	68.4(7)	107.4(9)
H(1)−Os−H(4)	71.2(5)	70.8(6)	57.4(9)
H(2)−Os−H(3)	84.1(5)	81.8(6)	62.2(10)
H(2)−Os−H(4)	76.2(5)	79.5(6)	101.4(10)
H(3)−Os−H(4)	132.6(5)	133.3(6)	136.5(9)
L−Os−H(2)−H(1)	9.7	3.3	
Ct−Os−H(1)−H(2)	11.0	3.7	
H(4)−H(1)−H(2)−H(3)			4.9
Ct−Os−H_2[b]	129.8	131.2	122.2

[a] L = P or As; Ct = centroid of the cyclopentadienyl ring. [b] The average of Ct−Os−H(1) and Ct−Os−H(2).

Scheme 2. Structural Parameters for the Osmium Complexes

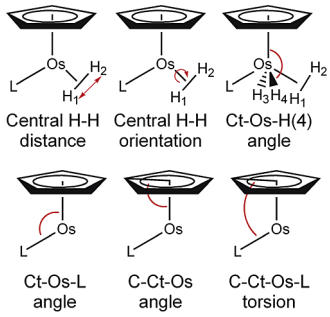

For the PCy_3 complex **3**, the DFT calculations reveal that there are multiple minima (Figure 3). The most stable structure (**3a**) is a tetrahydride in which the central H−H vector is *perpendicular* to the Ct−Os−L plane; this orientation differs from that seen for the PPh_3 complex **1** but agrees with the experimentally determined structure of **3**. The H···H distance of 1.68 Å is in the range expected for classical hydrides and is longer than the 1.31(3) Å distance measured experimentally. The next lowest energy structure (+0.72 kcal mol^{-1}) is also a tetrahydride (**3f**), but in this case the central H−H vector lies in the Ct−Os−L plane. The H···H distance in **3f** of 1.53 Å is suggestive of a weak (at best) interaction between these two atoms.

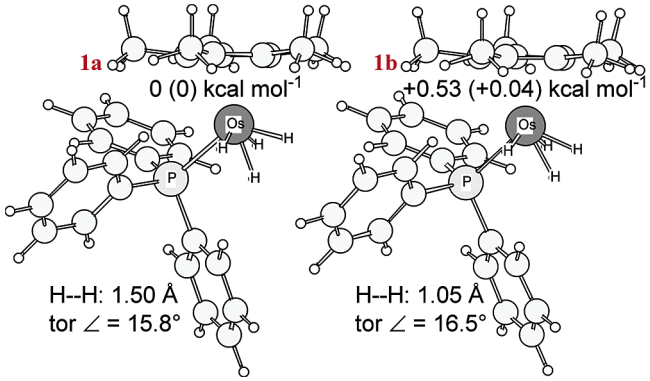

Figure 2. B3LYP/BS1 optimized structures and energies of the [Cp*OsH_4(PPh_3)]$^+$ complex, with the B3LYP/BS2 energies included in parentheses. The H···H distances listed are those calculated for the two central hydrogen atoms. The angles listed are the calculated C−Ct−Os−L angles. The calculated Ct−Os−L angles are 125.8° and 129.8° for **1a** and **1b**, respectively. The experimental values for the PPh_3 complex are 1.01 Å for the central H···H distance, 129.7° for the Ct−Os−L angle, and 16.8° for the C−Ct−Os−L angle.

A dihydrogen−dihydride minimum structure (**3b**) also exists, only 1.5 kcal mol^{-1} above the lowest energy tetrahydride structure, in which the H−H vector is still perpendicular to the Ct−Os−L plane; the H···H distance is 1.10 Å. Last, yet another tetrahydride minimum-energy structure (**3g**) exists (+0.23 kcal mol^{-1}) that perhaps would not be observed in the solid state because of crystal packing (Figure 4). In this isomer, the phosphine ligand is almost exactly trans to the centroid of the Cp* ring (Ct−Os−L angle is 171.6°) and the four hydrogen atoms are distributed symmetrically around the osmium (thus describing a local four-fold axis). This structure is similar to that observed for the isoelectronic pentahydride complex Cp^*OsH_5.[26]

The experimentally observed structure for the PCy_3 complex is closest to that of **3b**: in both structures the central H−H vector is perpendicular to the Ct−Os−L plane, and the Ct−Os−L angles are almost identical. The experimental H···H distance of 1.31 Å is somewhat longer than the 1.10 Å distance calculated for **3b**; it is possible (but we think unlikely) that the crystal studied consisted of an admixture of **3b** with small amounts of **3a**, which has a longer H···H distance.

Effect of the Ct−Os−L Angle on the Structures. The optimized structures of the various isomers of the osmium complexes [Cp*OsH_4(L)]$^+$ show an interesting relationship between the geometry adopted by the two central hydrogen atoms and the nature of the steric interactions between L and the Cp* ligand. In agreement with experiment, the calculated lowest energy structure of the PPh_3 complex has the vector of the two central hydrogen atoms parallel to the Ct−Os−L plane, whereas in the PCy_3 complex this vector is perpendicular to the Ct−Os−L plane. An overlay of the calculated structures of the PPh_3 and PCy_3 complexes (with osmium at the origin for both, the Os−L bonds exactly aligned, and the Ct−Os−L planes superimposed) reveals the steric influence of the PCy_3 ligand (Figure 5). Significantly, the Ct−Os−L angle is 129.7° in the PPh_3 complex but 139.0° in the PCy_3 complex, evidently owing to steric crowding in the latter complex between the Cp* and cyclohexyl groups. As discussed below, the steric crowding and/

(26) Gross, C. L.; Wilson, S. R.; Girolami, G. S. *J. Am. Chem. Soc.* **1994**, *116*, 10294−10295. Gross, C. L.; Girolami, G. S., unpublished observations.

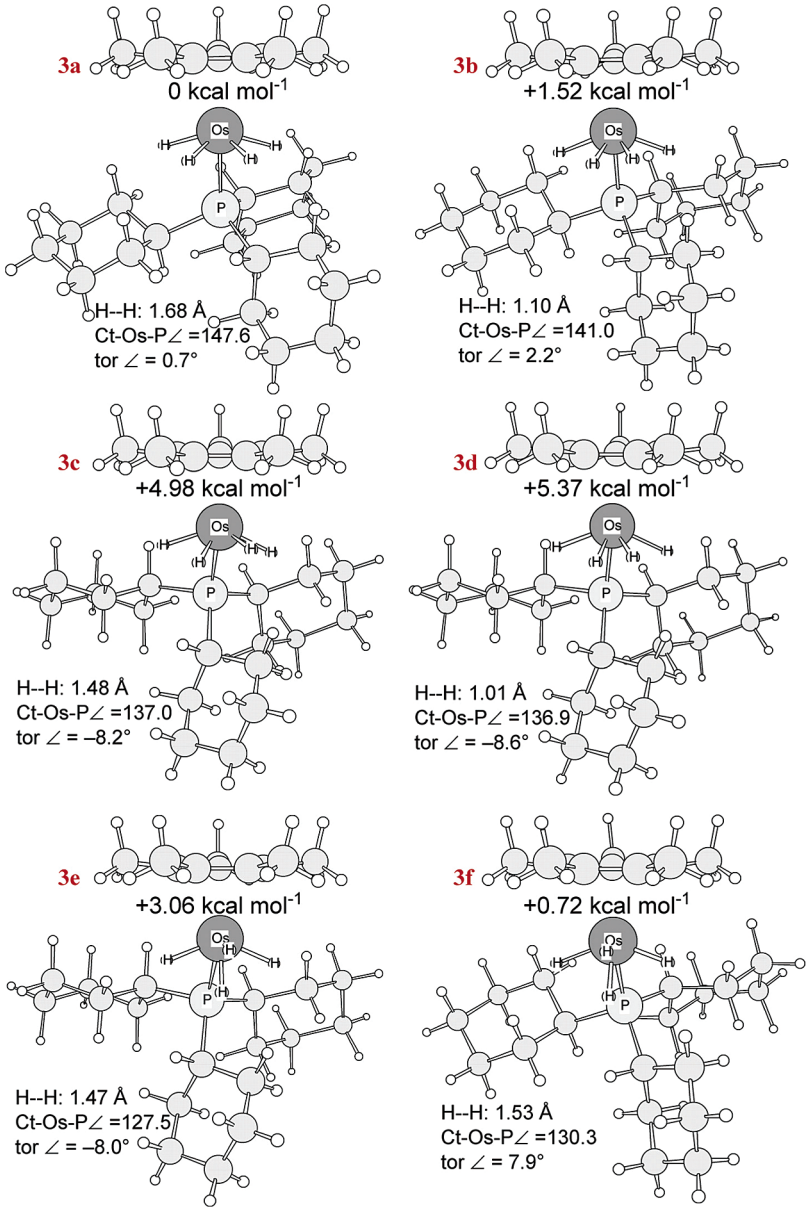

Figure 3. Six of the B3LYP/BS3 optimized structures of the $[Cp^*OsH_4(PCy_3)]^+$ complex. Relative energies are ΔE in kcal mol^{-1}. The H···H distances listed are those calculated for the two central hydrogen atoms. The torsion angles listed are the calculated C−Ct−Os−L angles. The experimental values for the PCy_3 complex are 1.31 Å for the central H···H distance, 139.0° for the Ct−Os−L angle, and −2.8° for the C−Ct−Os−L angle.

or the rehybridization of the metal−ligand bonding orbitals that attends this change in the Ct−Os−L angle could account for why the isomer in which the H_2 ligand is perpendicular to the Ct−Os−L plane is the lowest energy one for the PCy_3 complex.

Effect of the Orientation of the Cyclohexyl Groups in the PCy_3 Complex. To test the hypothesis that the large steric size of PCy_3 is responsible for the stabilization of the perpendicular orientation of the two central hydrogen atoms, the conformation of one of the cyclohexyl groups in the PCy_3 complex was altered to reduce the steric repulsions between it and the Cp* group. Specifically, the cyclohexyl substituent that is in closest contact with the Cp* ring was rotated (so that its methine hydrogen atom points toward the Cp* ring instead of away from it), and then the structure was reoptimized. This change, which causes the Ct−Os−L angle to become more acute by more than 10° (so that it is more similar to the 129.7° angle seen in the PPh_3 complex **1**), leads to a *reversal* in the relative stability of the in-plane vs perpendicular H_2 isomers. The isomer in which the central two hydrogen atoms lie parallel to the Ct−Os−L plane becomes slightly *lower* in energy than the isomer in which the H−H vector is perpendicular to the Ct−Os−L plane (Figure 3): compare **3c** and **3e** (ΔE_o = +4.21 and +3.08 kcal mol^{-1}, respectively) to **3a** and **3f** (ΔE_o = 0.0 and +0.72 kcal mol^{-1}, respectively). Of course, both of the isomers in which the cyclohexyl group is rotated are higher in energy than those in which it is oriented as seen in the experimentally determined structure. But the results again support the contention that steric effects (or their electronic consequences) govern which structure is most stable.

Effect of the BF_4^- Counterion on the Structure of the Complexes. Gusev has recently described the sensitivity of the nature of the H_2 ligand to weak intermolecular interactions in $IrH(H_2)Cl_2(PPr^i_3)_2$, a dihydrogen, hydride species.[27] To understand the influence of the BF_4^- anion on the observed structures

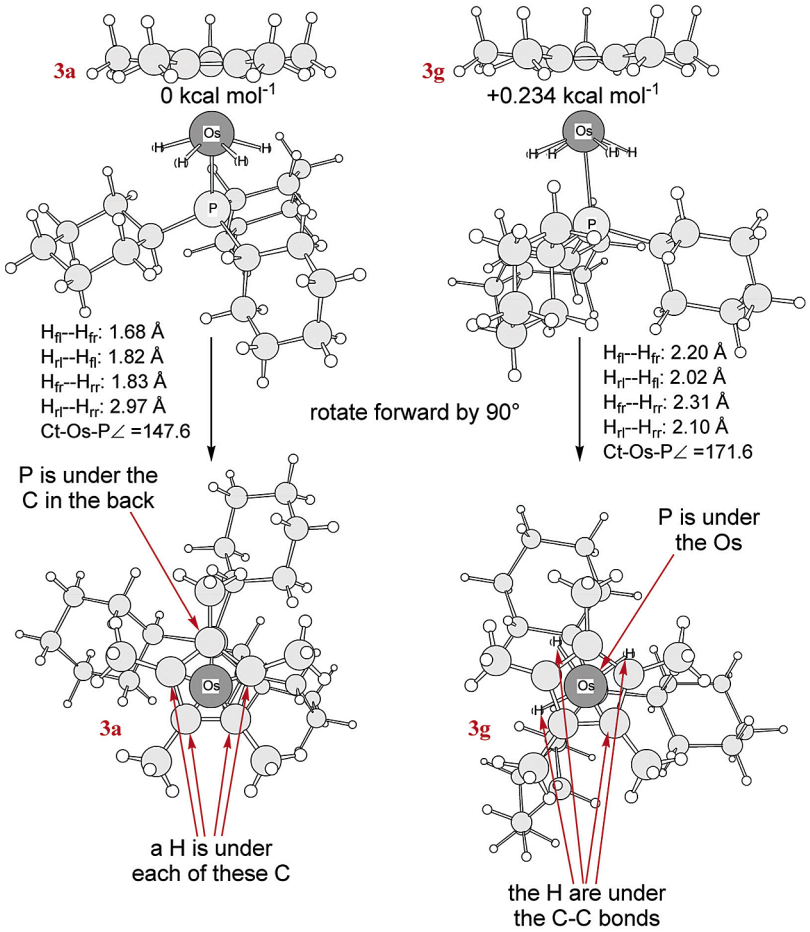

Figure 4. Comparison of a seventh B3LYP/BS3 optimized structure of the $[Cp^*OsH_4(PCy_3)]^+$ complex (**3g**) with that of the lowest energy structure (**3a**, which is very similar to that determined by neutron diffraction). Relative energies are ΔE in kcal mol^{-1}. The angles listed are the calculated Ct−Os−L angles. In the lowest energy structure, the Ct−Os−L angle is significantly less than 180°, whereas in the higher energy structure, the phosphine ligand is almost exactly trans to the centroid of the Cp* ring. The distances listed are the calculated H···H distances for the osmium-bound hydrogen atoms (H_{fr} is the hydrogen at the front right, H_{rr} is the hydrogen at the rear right, etc.).

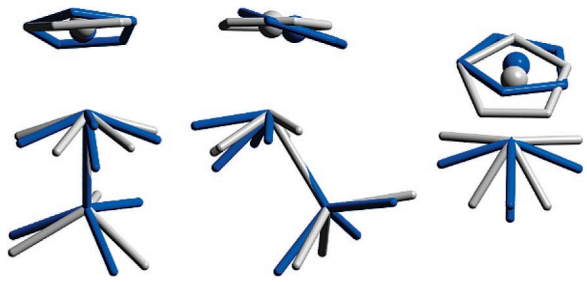

Figure 5. Alignment of the pruned B3LYP optimized structures of $[Cp^*OsH_4(PPh_3)]^+$ (blue) and $[Cp^*OsH_4(PCy_3)]^+$ (gray). The spheres represent the centroids of the Cp* rings.

of our complexes, we performed DFT geometry optimizations on the $[Cp^*OsH_4(PPh_3)]^+[BF_4]^-$ and $[Cp^*OsH_4(PCy_3)]^+[BF_4]^-$ ion pairs without constraints. In the crystal structure of the PPh_3 complex **1**, the BF_4^- anion lies near the $Os(H_2)$ ligand and is in contact with Cp* and PPh_3 hydrogen atoms of six other $[Cp^*OsH_4(PPh_3)]^+$ cations. Geometry optimization of the ion pair produces a single minimum-energy structure with an osmium-bound dihydrogen that has a slightly shorter H−H distance of 0.94 Å, compared to 1.05 Å for the free $[Cp^*OsH_4(PPh_3)]^+$ cation. In the optimized geometry, the BF_4^- anion occupies a calculated location similar to that in the crystal structure but closer to the Os center (Os···B calculated, 4.20 Å; Os···B crystal structure, 4.71 Å) (see Figure 6a). In the crystal structure of **3**, the BF_4^- anion lies to one side of the central $Os(H)_2$ ligand and is in contact with Cp* and PCy_3 hydrogen atoms of four other $[Cp^*OsH_4(PCy_3)]^+$ cations. Optimization of the geometry of the ion pair produces a single minimum-energy structure with four osmium-bound hydrides (just as for the free cation), but the two central hydrogens are brought closer together: the H···H distance is shorter (1.51 Å) when compared to the calculated structure of the free cation (1.68 Å) but still somewhat longer than that observed experimentally (1.31 Å). Again, the BF_4^- anion occupies a calculated location similar to that in the crystal structure but closer to the Os atom (Os···B calculated, 4.35 Å; Os···B crystal structure, 4.98 Å) (see Figure 6b). In general, including the BF_4^- anions in the geometry calculations tends to exaggerate the effect of ion pairing on the structures because, in the solid state, the anions interact with not just one cation but rather with several, so that their effect is diluted.

Vibrational Spectra and Hydride Dynamics. The INS vibrational spectra (T = 20 K) of $[Cp^*OsH_4(PPh_3)]BF_4$ and $[Cp^*OsD_4(PPh_3)]BF_4$ are shown in Figure 7a. Isotopic substitution of D for H makes the vibrational modes that involve mainly displacements of the D and D_2 ligands "invisible" in the INS spectrum relative to those involving H atoms. These types of

(27) Gusev, D. G. *J. Am. Chem. Soc.* **2004**, *126*, 14249−14257.

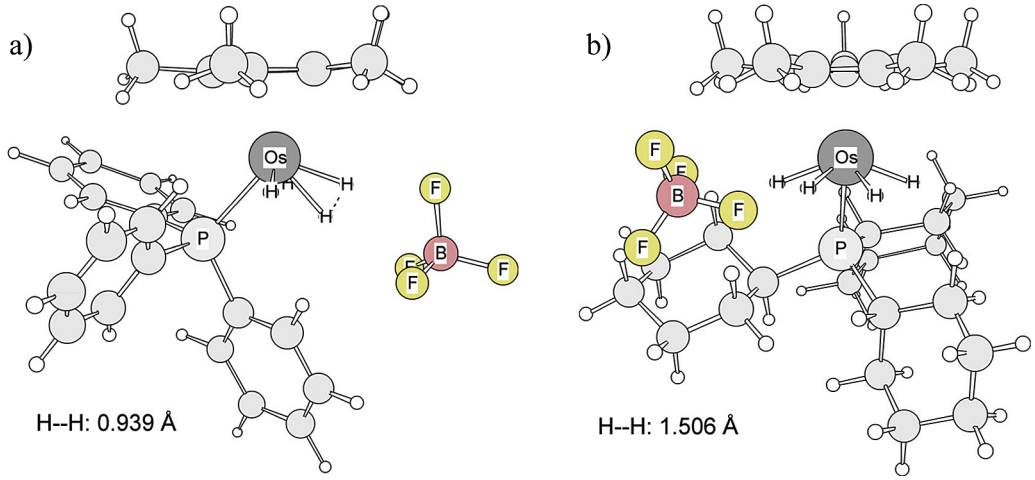

Figure 6. (a) B3LYP/BS1 optimized structure of the $[Cp^*OsH_4(PPh_3)]^+[BF_4]^-$ ion pair and (b) B3LYP/BS3 optimized structure of the $[Cp^*OsH_4(PCy_3)]^+[BF_4]^-$ ion pair. The H···H distances listed are those calculated for the two central hydrogen atoms. The experimental values for the PPh_3 and the PCy_3 complexes are 1.01 and 1.31 Å for the central H···H distances, respectively.

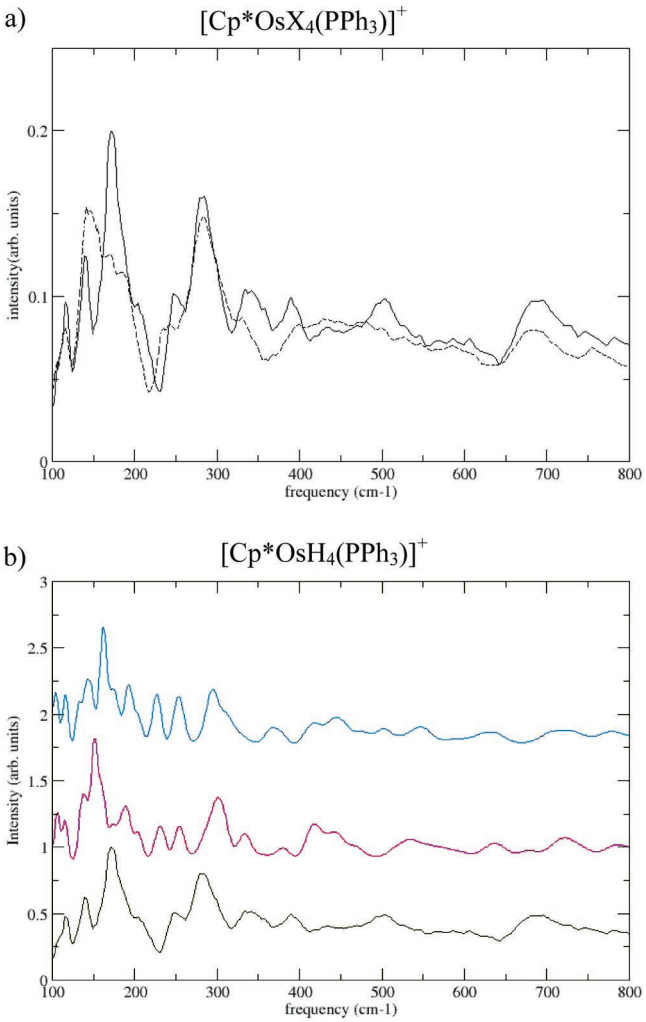

Figure 7. (a) Inelastic neutron scattering spectra of $[Cp^*OsH_4(PPh_3)][BF_4]$ (solid line) and $[Cp^*OsD_4(PPh_3)][BF_4]$ (dashed line) collected at 20 K. (b) Comparison of the experimental INS spectrum of $[Cp^*OsH_4(PPh_3)][BF_4]$ (bottom) with the INS spectra calculated for the two low-energy structures, $[Cp^*OsH_4(PPh_3)][BF_4]$ (**1a**, top) and $[Cp^*OsH_4(PPh_3)][BF_4]$ (**1b**, middle).

modes can therefore be readily identified. The actual nature of the particular mode must, however, be deduced from our computational study because the description of the vibrational modes for these types of large molecules can be rather complex.[28] Despite this complication, however, the frequencies of the modes involving the dihydrogen ligand can provide useful insights into the relative strengths of the metal−H and H···H interactions in the system.[29]

Several bands in the spectrum of the protio compound are (nearly) absent in the deuterio analogue, namely those at 172, 205, 335, 390, and 490 cm^{-1}. In contrast, a band at 145 cm^{-1} is more intense in the spectrum of the deuterio compound. As judged from the vibrational frequencies deduced from our computational study (see below), this latter band consists mainly of methyl torsions coupled with H−Os−H deformations, so that the decreased frequency of the D−Os−D motion shifts some of the accompanying intensity from the methyl torsion at 172 cm^{-1} to its counterpart at 145 cm^{-1}. The shoulder at 205 cm^{-1}, which disappears upon deuteration, probably corresponds to a calculated mode at the same frequency that is mainly H−Os−H deformation. As will be discussed below, on the basis of comparisons with the frequencies in the calculated spectrum of **1**, the peak in the experimental spectrum at 335 cm^{-1} is assigned to H···H torsional motion. The 390 cm^{-1} feature is best assigned to H−Os−H wagging motions, and the strong band in the INS spectrum at approximately 490 cm^{-1} should correspond to calculated modes at 478 and 501 cm^{-1} that are mainly rocking and/or wagging modes of the hydride and dihydrogen ligands. These values do not differ appreciably from those observed for other dihydrogen complexes.[28,30]

In Figure 7b the spectrum of the protio form is compared with calculated INS spectra (unscaled frequencies) for the two lowest energy isomers of the PPh_3 complex as determined from the DFT study: **1a** (classical tetrahydride structure) and **1b** (nonclassical structure with an H_2 ligand). Some of the low-frequency modes in the calculated spectrum are shifted with respect to those seen experimentally; the likely anharmonic nature of these modes may well account for some of this discrepancy. Those modes involving a significant degree of methyl torsion, on the other hand, may shift to higher frequen-

(28) Eckert, J.; Webster, C. E.; Hall, M. B.; Albinati, A.; Venanzi, L. M. *Inorg. Chim. Acta* **2002**, *330*, 240−249.
(29) Clot, E.; Eckert, J. *J. Am. Chem. Soc.* **1999**, *121*, 8855−8863.
(30) Kubas, G. J. *Metal−Dihydrogen and σ-Bond Complexes: Structure, Theory, and Reactivity*; Kluwer Academic Publishers: Norwell, MA, 2000; pp 245−249.

cies in the bulk solid because intermolecular interactions (which are neglected in our calculations on isolated molecules) tend to raise the rotational barriers for peripheral rotors.

These discrepancies aside, both calculated spectra roughly correspond with the experimental spectrum, but the calculated spectrum for the dihydrogen−dihydride isomer **1b** (which is the isomer observed crystallographically) is a somewhat better match. The agreement between the calculated and experimental spectra might be improved if the calculated spectrum was generated from an admixture of the dihydrogen−dihydride isomer and the slightly higher energy tetrahydride isomer; it is possible (but has not been established) that the two forms coexist at the data collection temperature of 20 K.

The dihydrogen torsional mode is found at 401 cm^{-1} in the harmonic calculation. However, the potential well for this mode (as for all motions with low or medium height rotational barriers) should be highly anharmonic, and one can calculate its frequency in a different way: in terms of a sinusoidal double-minimum potential for planar (one-dimensional) rotation used previously[31] for metal−dihydrogen complexes. From our calculated barrier to rotation (2.53 kcal mol^{-1}, see below) and the calculated H−H distance of 1.05 Å, this model predicts that the torsional mode should occur at 288 cm^{-1}, and that the corresponding ground rotational state tunnel splitting should be 0.050 cm^{-1}. Deviations of the potential from one that is purely sinusoidal could raise or lower the torsional mode frequency.[31]

The experimentally observed band that matches best with the H_2 torsional frequencies calculated above is the one that appears at 335 cm^{-1}. If one takes 335 cm^{-1} as the frequency of the torsional mode and uses the measured rotational constant B (for d(HH) = 1.01 Å, B = 31.5 cm^{-1}), a sinusoidal double-minimum potential for planar (one-dimensional) rotation provides an experimental barrier of 3.1 kcal mol^{-1}, which corresponds to a ground rotational state tunnel splitting of 0.028 cm^{-1}. These numbers are quite reasonable and lend support to the conclusion that the band at 335 cm^{-1}, which has no counterpart in the spectrum of the deuterio complex, is due to the dihydrogen torsion.

The 3.1 kcal mol^{-1} barrier for rotation of the H_2 ligand in $[Cp^*OsH_4(PPh_3)]^+$, as deduced from inelastic neutron scattering, compares well with the value obtained from density functional calculations. In the B3LYP/BS2 calculations (BS2 has triple-ζ plus double polarization on the metal-ligated hydrogen atoms), the $(H)_4$ and $(H_2)H_2$ isomers **1a** and **1b** are equal in energy, but are related by a calculated rotational barrier of 2.53 kcal mol^{-1}.

Effect of Steric Factors on the Electronic and Molecular Structure. The experimentally determined structures of the osmium complexes $[Cp^*OsH_4(L)]^+$, where L = PPh_3 (**1**), $AsPh_3$ (**2**), or PCy_3 (**3**), are snapshots along the oxidative-addition pathway shown in Scheme 1. For these osmium species, when the H−H axis of the dihydrogen ligand is parallel to the Ct−Os−L plane (as in **1** and **2**), the dihydrogen ligand is involved in π-back-bonding with a metal orbital consisting of a combination of d_{z^2} and d_{yz}. When the H−H axis is perpendicular to the Ct−Os−L plane (as in **3**), the dihydrogen ligand is involved in π-back-bonding with a metal orbital consisting largely of d_{xy} character. *We will now show that a change in the Ct−Os−L angle inverts the relative energies of the metal orbitals presented to the bound H_2.*

(31) Eckert, J.; Kubas, G. J. *J. Phys. Chem.* **1993**, *97*, 2378−2384.

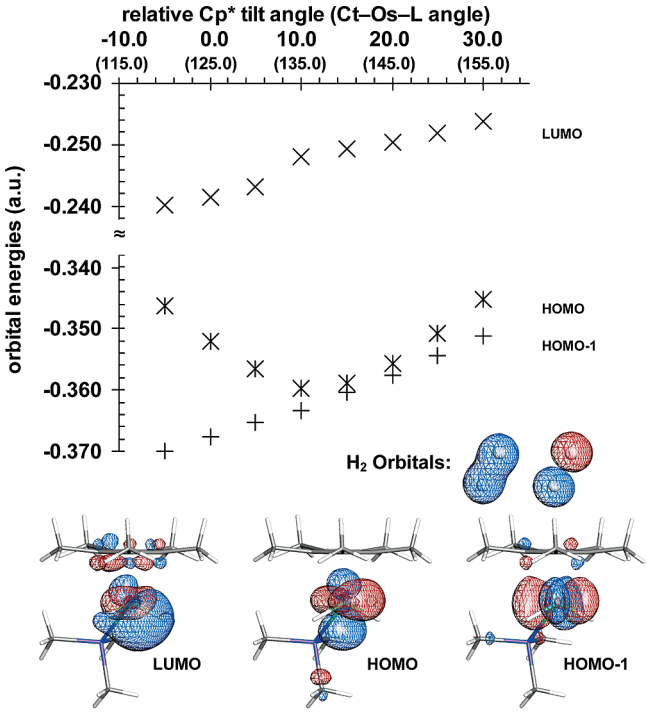

Figure 8. Orbital energies for the $[Cp^*OsH_2(PMe_3)]^+$ fragment as a function of the "relative Cp* tilt angle" and Ct−Os−L angle. A tilt angle of 0° corresponds to the natural Ct−Os−L angle (125°) of the minimum-energy fully optimized structure for the $[Cp^*OsH_4(PMe_3)]^+$ complex.[32]

Consider the hypothetical molecule $[Cp^*Os(H_2)H_2(PMe_3)]^+$ in a C_s geometry. Scanning the Ct−Os−L angle and allowing the other geometric variables to relax (by a constrained optimization, B3LYP/BS1) causes the HOMO and the second-highest occupied molecular orbital (HOMO−1) of the $Cp^*OsH_2PR_3$ fragment to change in relative energy (Figure 8).[32]

For the PPh_3 and $AsPh_3$ compounds **1** and **2**, in which the Ct−Os−L angle is ∼129° (in Figure 8), the HOMO is the d_{z^2}/d_{yz} hybrid. These orbitals project two lobes of opposite sign toward the empty coordination site, and both lobes lie in the Ct−Os−L plane. Thus, *the calculations predict (in agreement with experiment)* that π-back-bonding to the σ^* orbital of the H_2 ligand will be maximized (and the most stable structure will be formed) if the H−H vector for the dihydrogen ligand lies parallel to the Ct−Os−L plane.

For this same Ct−Os−L angle of ∼129°, the d_{xy} is the *second*-highest occupied molecular orbital (HOMO−1) and the HOMO/HOMO−1 energy gap is large (∼10 kcal mol^{-1}). This large gap means that there will be a strong preference for the H_2 ligand to lie parallel to the Ct−Os−L plane. In other words, HOMO−1, whose electrons are needed to stabilize the perpendicular H_2 orientation, is too low in energy to back-bond effectively into the σ^* orbital of the H_2 ligand, and as a result the perpendicular H_2 orientation is a transition state on the potential energy surface for the L = PPh_3 compound.

(32) For both the hypothetical $[Cp^*OsH_2(PMe_3)]^+$ fragment and the $[Cp^*OsH_4(PMe_3)]^+$ molecule, the relative orbital energies are essentially independent of the C−Ct−Os−P torsion angle (see Supporting Information). Therefore, we have plotted the results for only one C−Ct−Os−P torsion angle (0°). The Cp* tilt angle (defined as the deviation of the Ct−Os−P angle from its optimal value of 125° found calculationally) was fixed at various values and the remaining structural parameters were allow to relax (B3LYP/BS1). For each constrained $[Cp^*OsH_4(PMe_3)]^+$ optimized geometry, the two central hydrogen ligands were removed and the orbital energies for the resulting $[Cp^*OsH_2(PMe_3)]^+$ fragment were obtained from single-point B3LYP/BS1 calculations.

Decreasing the Ct−Os−L angle below 129° raises the energy of the HOMO and should cause stronger back-bonding to the H_2 ligand. Experimentally, the Ct−Os−L angle is smaller in the $AsPh_3$ complex **2** (128.5°) than in the PPh_3 complex **1** (129.7°). This result arises owing to the smaller steric size of the $AsPh_3$ ligand (the larger size of the As atom vs P places the phenyl substituents farther from the metal center, thus reducing the effective cone angle of the ligand). Thus, one might expect stronger back-bonding to the H_2 ligand (and a longer H···H distance) in the $AsPh_3$ complex than in the PPh_3 complex. The experimental H···H distances of 1.08(1) Å for L = $AsPh_3$ and 1.01(1) Å for L = PPh_3 are consistent with this hypothesis, and in contrast are not easy to explain on the basis of simple electron push−pull arguments.

Increasing the Ct−Os−L angle above 129° causes the two highest occupied molecular orbitals of the $[Cp^*OsH_2(PMe_3)]^+$ fragment to become closer in energy. For the tri(cyclohexyl)-phosphine complex $[Cp^*OsH_4(PCy_3)]^+$, the Ct−Os−P angle is ∼139° (Figure 8). For this geometry, the HOMO/HOMO−1 gap is small (∼2 kcal mol^{-1}). This small energy gap means that *both the parallel and perpendicular* orientations of the H_2 ligand correspond to minimum-energy structures on the potential energy surface.

Further insights into the orientation of the central H_2 ligand in these osmium complexes is provided by a theoretical analysis of four-legged piano-stool complexes conducted some years ago by Hoffmann and co-workers.[33] In their analysis, the p_π acceptor ability of a coordinated carbene with orientations shown in **I** and **II** was investigated. For structure **I**, overlap of the p_π orbital

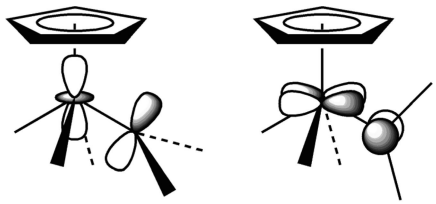

I **II**

with the metal d_{z^2} orbital is maximal at a Ct−M−C angle of 135°. For structure **II**, overlap with the metal d_{xy} orbital is maximal at a Ct−M−C angle of 90°. One conclusion to draw from this study is that (steric effects aside) the preferred orientation of the carbene acceptor orbital will change from being in the Ct−M−C plane at large Ct−M−C angles to being perpendicular to this plane at small Ct−M−C angles. Our experimental and theoretical investigations of complexes **1**−**3** are consistent with this analysis, where the H_2 σ^* antibonding orbital plays the role of the empty π acceptor orbital on the carbene ligand. As shown in Table 2, in the PPh_3 and $AsPh_3$ complexes **1** and **2**, where the σ^* acceptor orbital is in the Ct−Os−L plane, the Ct−Os−H_2 angle (reckoned to the midpoint of the H···H bond) is relatively large at ∼130°. In contrast, for the PCy_3 complex **3**, in which the σ^* orbital lies perpendicular to the Ct−Os−L plane, the Ct−Os−H_2 angle is smaller at ∼122°.

Hoffmann and co-workers also showed that the carbene acceptor orbital overlaps more strongly with orbital **II** than with orbital **I**. As a result, for our osmium complexes there should be more back-bonding to the H_2 ligand in the PCy_3 compound **3** (the analogue of structure **II**) than in the PPh_3 and $AsPh_3$ compounds **1** and **2** (the analogues of structure **I**). Because stronger back-bonding into the H_2 σ^* orbital should weaken and lengthen the H−H bond, the H···H distance should be longer in complex **3**. Experiment agrees with this conclusion: the H···H distance is 1.31(3) Å for L = PCy_3 but 1.01(1) and 1.08(1) Å for L = PPh_3 and $AsPh_3$, respectively.

Hydrogen Exchange Mechanisms. The neutron structures, the INS results, and the DFT calculations provide some insights into the possible dihydrogen/hydride exchange mechanisms in **1**−**3**. The INS and DFT calculations (as well as NMR studies)[2] clearly show that rotation of the H_2 ligand about its Os−H_2 bond is fast in all three complexes on the NMR time scale. For all three molecules, the isomer in which the H_2 ligand is oriented with its H−H vector perpendicular to the Ct−Os−L plane (as in the ground-state structure of **3**) is almost certainly important in the process that interchanges hydrogen atoms between the H_2 ligand and the "wing" classical hydride ligands. A similar intramolecular hydrogen exchange is observed in a series of iridium dihydrogen−dihydride complexes, $IrX(H_2)H_2(PR_3)_2$ (for X = Cl, Br, I and R = H, Me).[34] In these iridium systems, calculations indicate that the exchange mechanism involves rotation and oxidative addition of the dihydrogen ligand to form an intermediate tetrahydride complex. Similar effects are seen in the iron complex $Fe(H_2)H_2(PEtPh_2)_3$, for which an attractive cis-effect between dihydrogen and hydride ligand atoms has been proposed to be important in intramolecular hydrogen exchange.[35]

An alternative mechanism, involving the formation of a H_3 ligand, has been proposed to account for hydrogen exchange in the d^0 molybdenum complex $[CpMo(H_2)H_4(PMe_3)]^+$.[36] This mechanism is thought to operate in this complex because H_2 ligands attached to a d^0 metal center cannot undergo oxidative addition to form two hydride ligands. The tris(pyrazolyl)borate rhodium complexes $TpRh(H_2)H_2$ and $(Tp^{3,5Me})Rh(H_2)H_2$ are also thought to exchange by means of this mechanism, because the higher oxidation state structure generated by oxidative addition is too high in energy.[28] In contrast, the analogous iridium complex, $TpIrH_4$, which can support the higher oxidation state, can exchange by means of the oxidative addition mechanism.[37]

Variable-temperature ^1H NMR studies of complexes **1**−**3** show that the four Os−H hydrogen atoms are exchanging with one another: the room-temperature ^1H NMR spectra all feature a single resonance for the four Os−H groups.[2] For the PPh_3 and PCy_3 compounds **1** and **3**, the resonances remain sharp down to approximately −100 °C, at which point they begin to broaden. Even at −140 °C, however, the resonances for **1** and **3** remain broad singlets. In contrast, the hydride resonance for the $AsPh_3$ complex **2** decoalesces by −140 °C into two broad, equal-intensity features separated by 1.0 ppm. From this chemical shift separation and the coalescence temperature, an activation energy for the dihydrogen/hydride exchange process of ∼6.0 kcal mol^{-1} was calculated.[2]

(33) Kubáček, P.; Hoffmann, R.; Havias, Z. *Organometallics* **1982**, *1*, 180−188.
(34) Li, S.; Hall, M. B.; Eckert, J.; Jensen, C. M.; Albinati, A. *J. Am. Chem. Soc.* **2000**, *122*, 2903−2910.
(35) Van Der Sluys, L. S.; Eckert, J.; Eisenstein, O.; Hall, J. H.; Huffman, J. C.; Jackson, S. A.; Koetzle, T. F.; Kubas, G. J.; Vergamini, P. J.; Caulton, K. G. *J. Am. Chem. Soc.* **1990**, *112*, 4831−4841.
(36) Bayse, C. A.; Hall, M. B.; Pleune, B.; Poli, R. *Organometallics* **1998**, *17*, 4309−4315.
(37) Webster, C. E.; Singleton, D. A.; Szymanski, M. J.; Hall, M. B.; Zhao, C.; Jia, G.; Lin, Z. *J. Am. Chem. Soc.* **2001**, *123*, 9822−9829.

DFT calculations show that there are no low-energy structures in which the H_2 ligand is bound to one of the "wing" coordination sites. Therefore, such intermediates can be ruled out as being important to the exchange mechanism. Instead, hydrogen exchange most likely occurs through oxidative addition to form tetrahydride intermediates, or through transition states that directly exchange one of the H_2 hydrogen atoms with one of the hydrides through a concerted rotation/bond-breaking transition state. If tetrahydride intermediates are involved, one possible exchange mechanism is via the symmetric isomer (L exactly trans to Cp*) depicted in Figure 4. The ~6.0 kcal mol^{-1} barrier for dihydrogen/hydride exchange found experimentally is certainly consistent with the energy differences found by DFT between the ground-state structure and various higher energy structures with tetrahydride character.

Acknowledgment. Work at the University of Illinois at Urbana−Champaign was supported by the National Science Foundation (Grant Nos. CHE 00-76061 and CHE 04-20768). Work at Argonne National Laboratory was supported by the U.S. Department of Energy, Office of Basic Energy Sciences, Division of Materials Sciences, under Contract No. W-31-109-ENG-38. Work at Texas A&M University was supported the National Science Foundation (Grant Nos. CHE 98-00184 and MRI 02-16275) and the Welch Foundation (Grant No. A-648). Work at the Lujan Center of Los Alamos National Laboratory, a National User Facility, was supported by the Office of Science, U.S. Department of Energy. The authors also thank Josiah Manson for a Cerius^2 SDK implementation of an interface between Cerius^2 and POV-Ray, a ray tracer (used in the production of Figure 5).

Supporting Information Available: CIF files for the structural determination of compounds **1**−**3**; Cartesian coordinates of the optimized structures of **1a**, **1b**, and **3a**; an overlay figure of the computed $[Cp^*OsH_2(PMe_3)]^+$ fragments (for Figure 8) with the lowest energy fully optimized geometries of $[Cp^*OsH_4(PPh_3)]^+$ and $[Cp^*OsH_4(PCy_3)]^+$; plots of the orbital energies as a function of the Ct−Os−L angle for both orientations of the Cp* ring for the hypothetical $[Cp^*OsH_2(PMe_3)]^+$ fragment; schemes for the possible hydrogen exchange mechanisms; and full references for citations with more than 10 authors. This material is available free of charge via the Internet at http://pubs.acs.org.

JA052336K